

Removal of congo red azo dye from aqueous solution by ZnO nanoparticles loaded on multiwall carbon nanotubes

Seyed Masoud Seyed Arabi^{a,**}, Rahman Shakibaei Lalehloo^a, Mohamad Reza Talei Babil Olyai^b, Gomaa A.M. Ali^{c,d}, Hamidreza Sadegh^{e,*}

^a Department of Chemistry, Karaj Branch, Islamic Azad University, Karaj, Iran

^b Department of Chemistry, South Tehran Branch, Islamic Azad University, Tehran, Iran

^c Chemistry Department, Faculty of Science, Al-Azhar University, Assiut 71524, Egypt

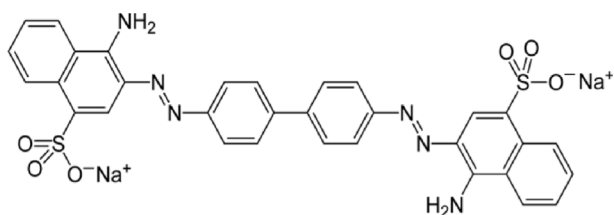
^d Faculty of Industrial Sciences & Technology, Universiti Malaysia Pahang, Gambang, 26300 Kuantan, Malaysia

^e West Pomeranian University of Technology, Szczecin, Faculty of Chemical Technology and Engineering, Institute of Inorganic Chemical Technology and Environment Engineering, ul. Pułaskiego 10, 70 - 322 Szczecin, Poland

ABSTRACT

The present work investigates the performance of ZnO nanoparticles loaded on multiwall carbon nanotubes for removing of congo red dye from aqueous solutions. The prepared nanocomposites are characterized by XRD, TEM, FTIR, FESEM and EDX. The effect of various parameters such as contact time, temperature and adsorbent dosage are investigated and discussed. The obtained results show that the optimum adsorption conditions are contact time of 50 min., 55 °C and dosage of 9 mg. These optimum parameters give a high removal ratio of 99.8%. The adsorption data were well fitted by pseudo-second-order model. The obtained results reveal that ZnO/MWCNTs is a promising, environmentally friendly and efficient adsorbent for some wastewater treatment.

Keywords: Congo red; ZnO nanoparticles; Adsorption; Carbon nanotubes; Nanoadsorbent



Scheme 1. Congo red structure.

synthesis of the ZnO/MWCNTs nanocomposites, and characterized by XRD, TEM, FTIR, FESEM and EDX techniques. The composite performance for the adsorption of congo red was studied and the effect of different parameters including contact time, temperature and adsorbent dosage on the adsorption performance was investigated in detail. Adsorption kinetic analysis was carried out to investigate further into the adsorption process.

2. Experimental procedure

2.1. Materials

Congo red (CR) is a sodium salt of benzidine diazo-bis-1-naphthylamino-4-sulfonic acid. Its chemical structure is shown in Scheme 1 and it is used as a biological substance and acid-base indicator. The absorption of CR in aqueous solution (pH = 7) takes place at 497 nm [17,28]. ZnO is a white powder mineral compound and it is found in nature as zingit Connie which contains an especial amount of manganese and other impurities creating a reddish yellow color. ZnO is a thermo-chromic crystal that is under the influence of heat its white color changes into yellow which reversible in cold and exposure to air. The MWCNTs (average diameter: 20–30 nm, length > 2 μm, purity > 97%, specific surface area: 160–200 m²/g) and nitric acid were purchased from Sigma (USA).

2.2. Applications

In the study, CR with a molecular mass of 407.979 g/mol was used to prepare the aqueous solution. In 30 mL of CR color solution, various amounts (1–9 mg) of adsorbents were used to study the effect of dosage. In addition, different contact times and concentrations were studied. After this, the soluble and adsorbent species were separated from each other by a nanofilter paper. Adsorption measurements were carried out by the UV-Vis device at 497 nm. After detected the concentration of CR, the adsorbed amount (q (mg g⁻¹)) and removal percentage (%) were calculated using the following equations [24,29,30]:

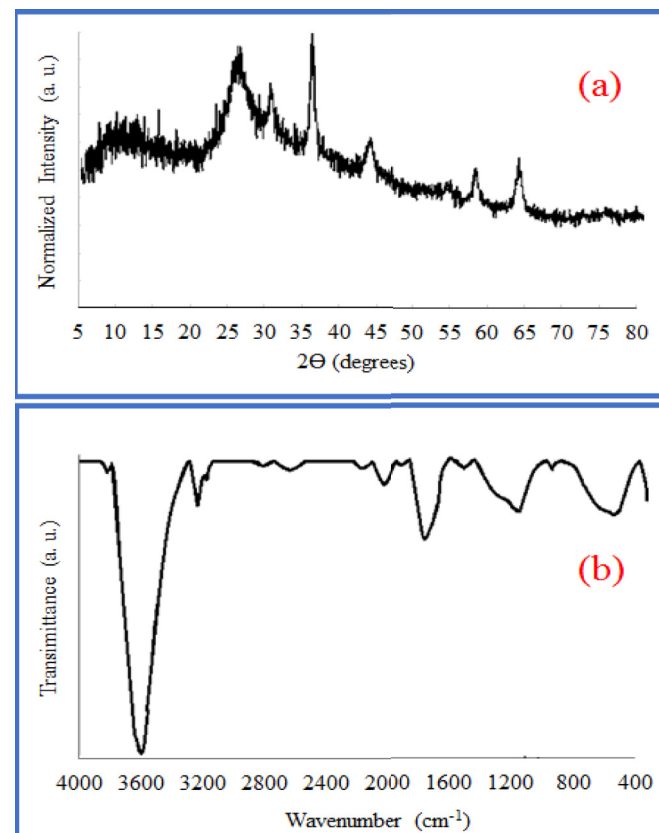


Fig. 2. XRD pattern (a) FTIR spectrum (b) ZnO nanoparticles.

$$q_e = \frac{(C_o - C_e)V}{m} \quad (1)$$

$$\text{Removal} = \frac{C_o - C_t}{C_o} \times 100 \quad (2)$$

where C_o , C_e and C_t (mg/L) are the liquid-phase concentrations of CR at initial, equilibrium and time (t), respectively. V is the volume of the solution (L) and m is the mass (g) of the adsorbent used. All the experiments were performed in triplicate, and the mean values have been used in calculations.

2.3. Preparation of ZnO nanoparticles and ZnO/MWCNTs nanocomposites

Isopropanol solvent (32.5 mL) and monoethanolamine (1.2 mL)

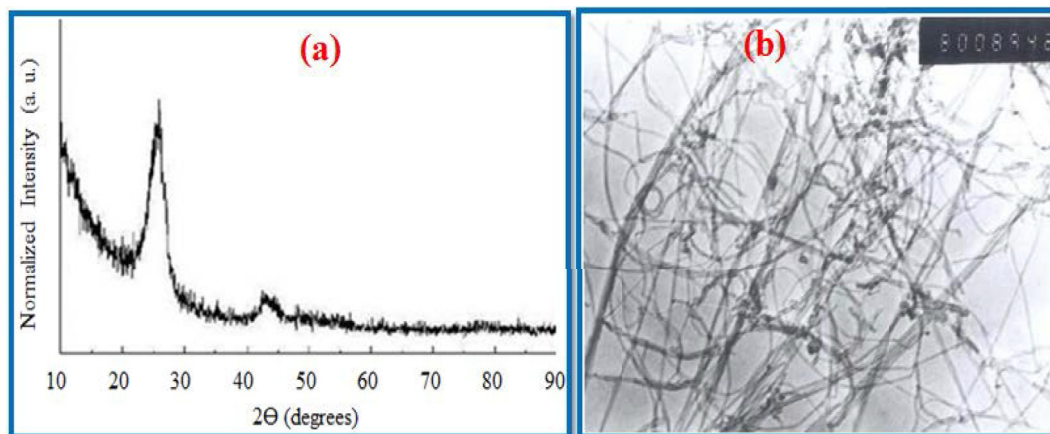


Fig. 1. XRD pattern (a) and TEM image (b) of MWCNTs.

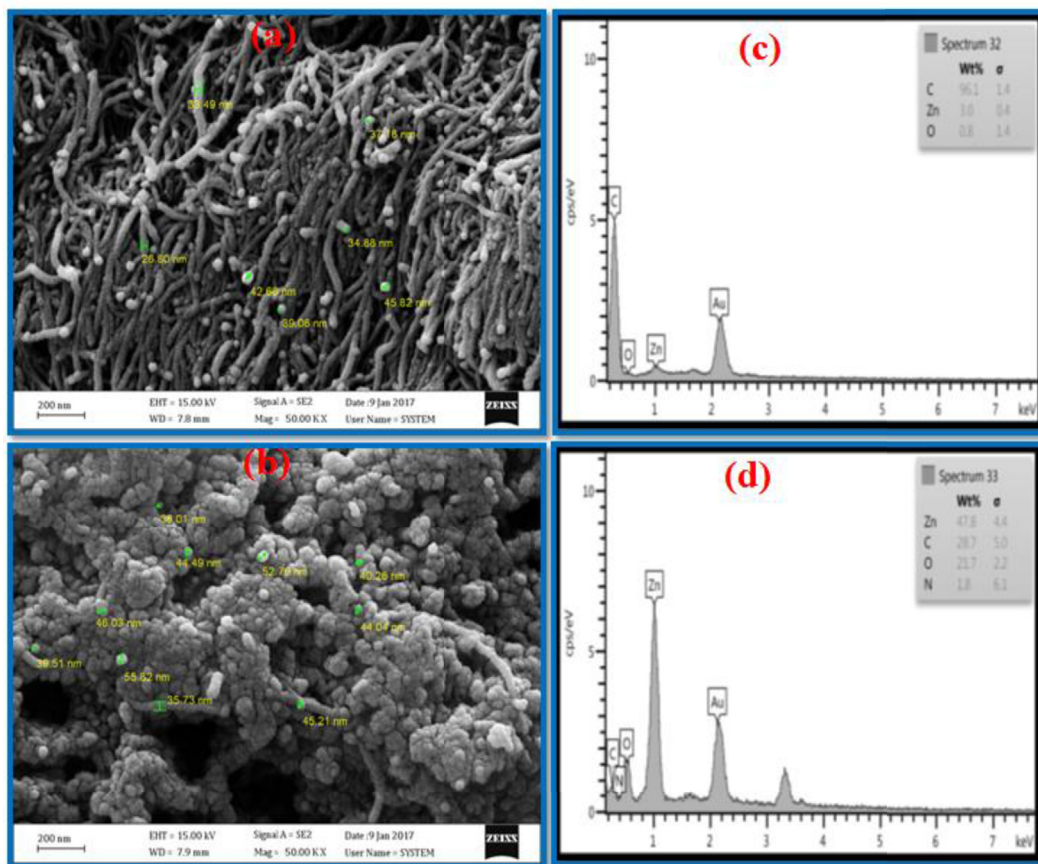


Fig. 3. FESEM images (a, b) and EDX analyses (c, d) for ZnO(D)/MWCNTs and ZnO(AC)/MWCNTs, respectively.

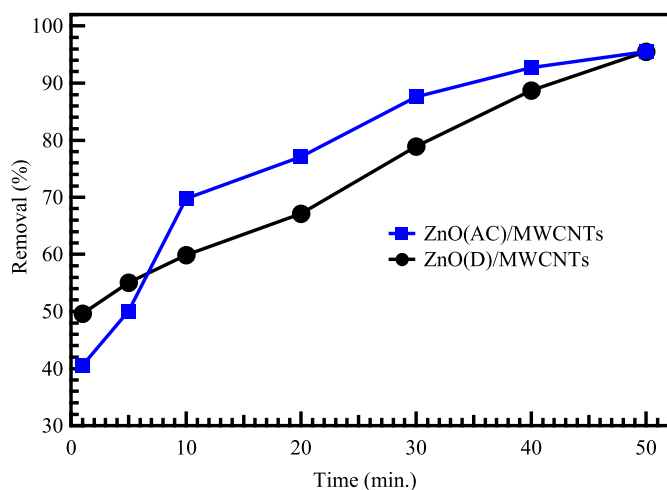


Fig. 4. Time optimization for CR adsorption on ZnO(D)/MWCNTs and ZnO(AC)/MWCNTs.

were used to dissolve dehydrated zinc oxide (3.012 g). The solution was heated at 75 °C and rotated magnetically for 1 h to produce a homogenous solution. The solution was kept for 24 h at room temperature. Then the constant and stable solution was heated up slowly to 82 °C and stirred by a magnetic mixer to vaporize the solution into a homogenous and viscous gel. After 24 h, the final gel was heated at 550 °C in a furnace for 2 h. The obtained material was coded as ZnO(D).

For ZnO loading on MWCNTs, MWCNTs were merged in a complex solution of HCL and HNO₃ with 1:1 proportion to remove their impurities. Then it is heated in an oven under 50 °C for 12 h. Then 0.1 g of

nanotubes and 0.1 g of ZnO were mixed with 5 mL of ethanol and 2 mL of distilled water for 12 h by a powerful mixer, then was kept in ultrasonic for 4 h and for 12 h in reflux in 75 °C. The obtained nanocomposite was coded as ZnO(D)/MWCNTs.

In another procedure, dehydrated zinc acetate (0.735 g) and potassium hydroxide (0.369 g) were dissolved in 32 mL and 16 mL of methanol, respectively. Then the potassium hydroxide solution was added to zinc acetate solution dropwise under stirring by a powerful mixer while the temperature of the solution is kept on 60 °C. The solution is left for 2 h. The resultant sediments were mixed with 12.5 mL of methanol and 2.5 mL of chloroform. Then the nanoparticles mixed in chloroform are put in the ultrasonic unit, thereafter the solution was kept in a nitrogen atmosphere for 12 h and finally transferred into a drying oven for 3 h. The obtained material was coded as ZnO(AC). Then, ZnO nanoparticles dissolved in chloroform were kept in the ultrasonic unit for 2 h and then 0.1 g of MWCNTs were put in the ultrasonic unit. After mixing, the mixture was put in a nitrogen atmosphere and finally dried for 3 h. The obtained nanocomposite was coded as ZnO(AC)/MWCNTs.

2.4. Characterizations

Phase structure and crystallinity of were identified by X-ray diffraction (XRD) using PANalytical X'Pert Pro MPD X-ray diffraction with monochromatic Cu-K_α radiation, tube voltage of 40 kV, tube current of 40 mA and scanning range 2θ = 10–70°. Transmission electron microscopy (TEM) images were taken on a 100 kV JEOL JEM-1010 microscope operated with AMT image capture engine software. The FTIR spectra were analyzed using PerkinElmer Spectrum 100 FT-IR spectrometer in the range of 4000–400 cm⁻¹. FE-SEM images were collected using scanning electron microscope (Zeiss EVO MA-10 SEM operating

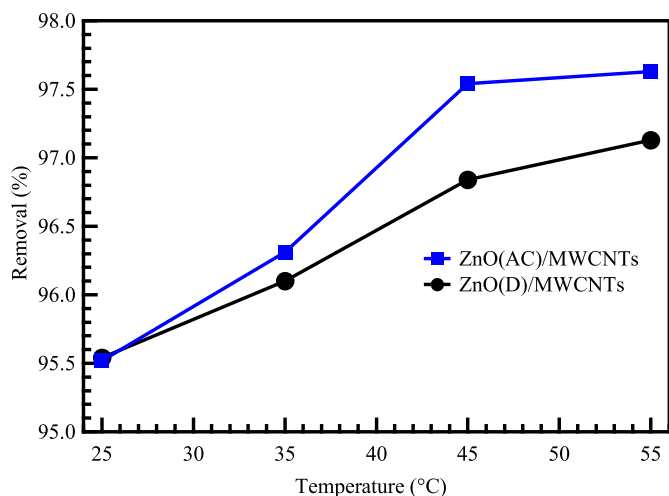


Fig. 5. Temperature optimization for CR adsorption on ZnO(D)/MWCNTs and ZnO(AC)/MWCNTs.

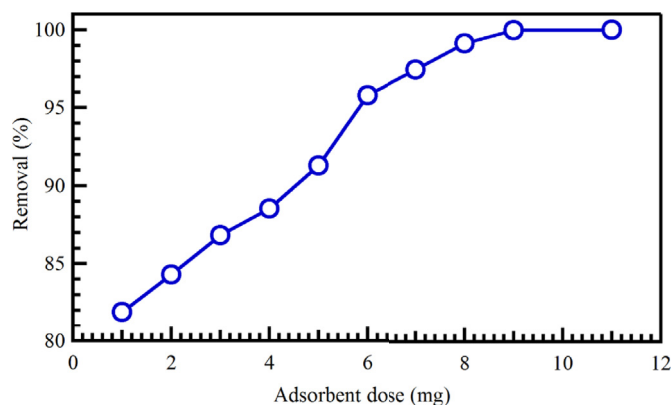


Fig. 6. Dosage optimization for CR adsorption on ZnO(AC)/MWCNTs.

at 10.0 keV).

3. Results and discussion

3.1. Structural and morphological properties

Fig. 1a shows the phase structures of the MWCNTs. It displays the strong diffraction peak at 26.4° could be attributed to the disordered (0 0 2) stacking layers and the typical pattern of amorphous carbon, indicating the MWCNTs structure. Another important characterization method for evaluating the characteristic of MWCNTs is the transmission electron microscopy (TEM) as shown in Fig. 1b. It evidently shows a general view of MWCNTs agglomerated and the fibers were tangled.

XRD of ZnO nanoparticles was also analyzed and the pattern of ZnO (Fig. 2a) indicates the polycrystalline nature of the ZnO nanoparticles and the peaks were indexed to (100), (002), (101), (110) and (103) with respect to standard ICDD card no: 36–1451 [31]. The FTIR spectrum of ZnO nanoparticles is shown in Fig. 2b and the following peaks were observed: 493 and 535 cm^{-1} (Zn–O stretching vibrations), 942 cm^{-1} (stretching of Zn–OH groups), 1646 and 3466 cm^{-1} (stretching and bending vibrations of O–H group), 2955 (stretching modes of C=O) and 3435 cm^{-1} (O–H stretching vibrations).

The FE-SEM images of ZnO(D)/MWCNTs and ZnO(AC)/MWCNTs are presented in Fig. 3a and b. The composites demonstrate a good dispersion of the samples which are entangled one on the other with a larger exposed surface making the material very suitable for adsorption. In addition, it revealed that the samples have a uniform distribution of

ZnO nanoparticles of $\sim 25\text{--}45\text{ nm}$ for ZnO(D)/MWCNTs and $\sim 35\text{--}45\text{ nm}$ for ZnO(AC)/MWCNTs. Furthermore, FESEM shows ZnO nanoparticles loaded on the surface of MWCNTs to form an evenly three-dimensional network like nanostructure and the morphology of both samples are in keeping with that of MWCNTs. By comparison, ZnO (D)/MWCNTs consists of spherical particles with poor agglomeration and aggregation takes place during the particle growth process, while the external surface of the sample ZnO(AC)/MWCNTs has a large number of particle size with spherical morphology.

The overall characterization results confirmed the formation of a microcrystalline rough surface morphology on CNTs and the agglomeration of the particles was seen in the FE-SEM images. Moreover, ZnO is well dispersed on the CNTs surface in both samples, although some aggregated ZnO are still visible while most parts exhibited the formation of irregular islands in MWCNTs surfaces [19,32]. The particle was found spherical in shape and surface morphology was found homogenous in specific regions. This is because the functional group was attached by ZnO adding experiment, which increased the number of attached in the modified surfaces. However, to confirm that quantitative analyses of C, Zn, O and N were performed by EDX for the ZnO (D)/MWCNTs and ZnO(AC)/MWCNTs samples and shown in Fig. 3c and d. The percent of all elements in both samples is confirmed by EDX. In addition, it was found that ZnO(D)/MWCNTs consists of 96.1% C, 3.0% Zn and 0.8% O. On the other hand, 47.5% Zn, 28.7% C, 21.7% O and 1.8% N for ZnO(AC)/MWCNTs sample as shown in the insets of Fig. 3c and d.

3.2. Adsorption properties

3.2.1. Effects of contact time

The adsorption time is one of the most important indexes for the adsorption performance in wastewater treatment systems because it can describe the process of adsorption and elucidate the possible adsorption mechanism of sorption reactions. The effect of contact time on the adsorption of CR is shown in Fig. 4. Although, the two samples exhibited the adsorption rate was quite fast during the first 10 min and after that became slower gradually, with adsorption equilibria reached within 50 min. Also, the adsorption capacity increases rapidly at the initial stage for the entire sample and reaches equilibrium quickly. In addition, ZnO(AC)/MWCNTs has a higher adsorption capacity than ZnO(D)/MWCNTs.

There is a considerable difference between CR adsorption and various contact time due to the presence of a large number of active sites on the surface of ZnO(AC)/MWCNTs at the beginning of adsorption, so the adsorption rate is faster than ZnO(D)/MWCNTs. The dye molecules reach the boundary layer then they propagate on the adsorbent surface. Then, they are distributed in the porous structure of the adsorbent and this phenomenon becomes longer proportional to time. Finally, all the active sites are occupied, the adsorption reached equilibrium, and the adsorption capacity is not changed.

3.2.2. Effect of temperature

The adsorption capacity of ZnO(D)/MWCNTs and ZnO(AC)/MWCNTs increases from 95.6 to 97.6% with increasing the temperature from 25 to 55°C (as shown in Fig. 5), indicating clearly that CR is adsorbed endothermic on to both adsorbents. Its means, with the increase in temperature, the molecular movement will increase too which will increase the total energy of adsorbent molecules.

3.2.3. Effect of adsorbent dosage

The dosage of the adsorbent is an important and effective factor in surface adsorption processes and adsorption capacity is determined by the initial concentration of adsorbent in practical conditions. The effect of adsorbent dose is shown in Fig. 6. As could be seen, the removal rate increased from 82.0% to 99.8% when the amount of ZnO(AC)/MWCNTs increased from 1 mg to 9 mg. Beyond 9 mg as dosage there is

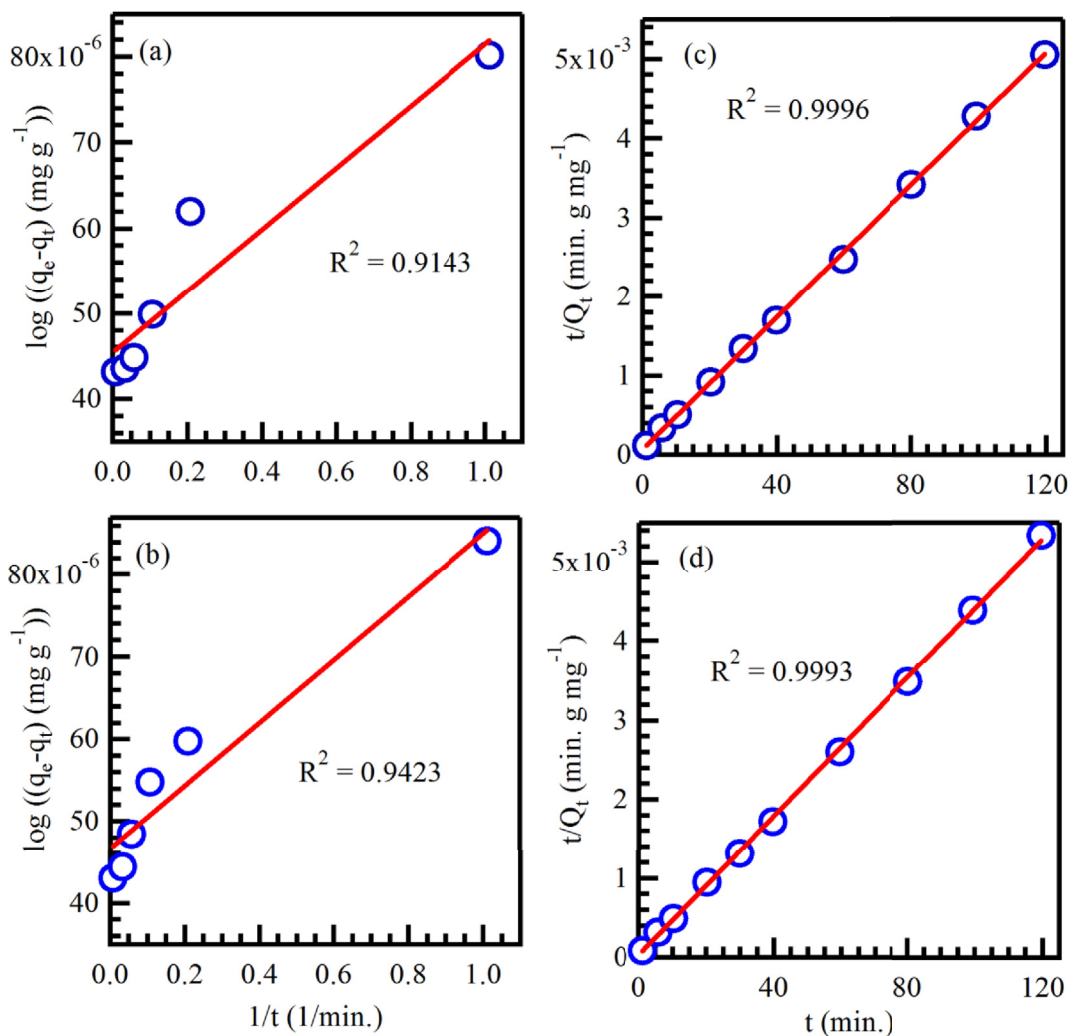


Fig. 7. Pseudo-first-order (a, b) and pseudo-second-order (c, d) kinetics for ZnO(D)/MWCNTs and ZnO(AC)/MWCNTs, respectively.

Table 1
Kinetic parameters for the CR adsorption on ZnO(D)/MWCNTs and ZnO(AC)/MWCNTs.

Adsorbent	Pseudo-first-order model			Pseudo-second-order model		
	q_e (mg g ⁻¹)	k_1 (min ⁻¹)	R ²	q_e (mg g ⁻¹)	k_2 (g mg ⁻¹ min ⁻¹)	R ²
ZnO(D)/MWCNTs	117.25	0.065	0.9143	119.32	0.179	0.9996
ZnO(AC)/MWCNTs	243.03	0.789	0.9423	249.51	0.129	0.9993

Table 2
CR adsorption capacities and removal percentages different adsorbents.

Adsorbent	Adsorbate	Adsorption capacity (mg g ⁻¹)	Removal (%)	Reference
Coir pith carbon	CR	6.70	70.0	[36]
Anilinepropylsilica xerogel	CR	22.62	77.4	[37]
Commercial anion exchange membranes (EBTAC)	CR	11.01	98.0	[38]
Halloysite-magnetite-based composite	CR	80.78	99.3	[39]
Rice husk carbon activated by steam	CR	-	99.0	[40]
Local natural clay	CR	74.62	95.63	[41]
ZnO/MWCNTs	CR	249.51	99.8	This work

no adsorption took place. This development in surface adsorption results in an increase in adsorbent concentration and an increase in the number of available and active sites for color ions as shown in Fig. 6.

3.2.4. Adsorption kinetics

For further investigation on the mechanisms of CR adsorbed onto ZnO(D)/MWCNTs and ZnO(AC)/MWCNTs, the data were fitted to pseudo-first-order [10,24,33] and pseudo-second-order [29,34,35] can be written as Eqs. (3) and (4), and the data from both models are shown

in Fig. 7.

$$\log(q_e - q_t) = \log q_e - \frac{k_1}{2.303} t \quad (3)$$

$$\frac{t}{q_t} = \frac{1}{k_2 q_e^2} + \frac{t}{q_e} \quad (4)$$

where q_e and q_t stand for the adsorbed amount of CR at equilibrium and time t , respectively. k_1 and k_2 are pseudo-first-order (min^{-1}) and pseudo-second-order rate constants, respectively. The obtained values were listed in Table 1. Based on the R^2 values pseudo-second-order rate model was found to be the best fitting of the experimental data [36]. The removal efficiencies of different adsorbents toward CR removal are compared as listed in Table 2.

4. Conclusion

In the study, congo red dye is omitted from wastewater and aqueous solutions by adsorption on ZnO/MWCNTs. With the increase of all different parameters such as the amount of adsorbent, solution temperature, the time the rate of adsorption increased. Contact time of 50 min., temperature of 55 °C and dosage of 9 mg were chosen as the optimum adsorption conditions. These optimum parameters give a high removal ratio of 99.8%. The results of the present study revealed that ZnO/MWCNTs nanocomposite is a good candidate for dyes removal and wastewater treatments.

Appendix A. Supplementary data

Supplementary data to this article can be found online at <https://doi.org/10.1016/j.physe.2018.10.030>.

References

- A.L. Cazetta, A.M.M. Vargas, E.M. Nogami, M.H. Kunita, M.R. Guilherme, A.C. Martins, T.L. Silva, J.C.G. Moraes, V.C. Almeida, NaOH-activated carbon of high surface area produced from coconut shell: kinetics and equilibrium studies from the methylene blue adsorption, *Chem. Eng. J.* 174 (2011) 117–125.
- A. Gundogdu, C. Duran, H.B. Senturk, M. Soyhlak, D. Ozdes, H. Serencam, M. Imamoglu, Adsorption of phenol from aqueous solution on a low-cost activated carbon produced from tea industry waste: equilibrium, kinetic, and thermodynamic study, *J. Chem. Eng. Data* 57 (2012) 2733–2743.
- S. Hashemian, A. Foroghmoqhadam, Effect of copper doping on CoTiO₃ ilmenite type nanoparticles for removal of congo red from aqueous solution, *Chem. Eng. J.* 235 (2014) 299–306.
- T.-H. Kim, C. Park, J. Yang, S. Kim, Comparison of disperse and reactive dye removals by chemical coagulation and Fenton oxidation, *J. Hazard Mater.* 112 (2004) 95–103.
- L. Szpyrkowicz, C. Juzzolino, S.N. Kaul, A Comparative study on oxidation of disperse dyes by electrochemical process, ozone, hypochlorite and fenton reagent, *Water Res.* 35 (2001) 2129–2136.
- N.M. Mahmoodi, Photocatalytic ozonation of dyes using copper ferrite nanoparticle prepared by co-precipitation method, *Desalination* 279 (2011) 332–337.
- A. Ahmad, S. Puasa, M. Zulkali, Micellar-enhanced ultrafiltration for removal of reactive dyes from an aqueous solution, *Desalination* 191 (2006) 153–161.
- E. Alventosa-deLara, S. Barredo-Damas, M. Alcaina-Miranda, M. Iborra-Clar, Ultrafiltration technology with a ceramic membrane for reactive dye removal: optimization of membrane performance, *J. Hazard Mater.* 209 (2012) 492–500.
- S. Agarwal, H. Sadegh, M. Monajjemi, A.S. Hamdy, G.A.M. Ali, A.O. Memar, R. Shahryari-ghoshekandi, I. Tyagi, V.K. Gupta, Efficient removal of toxic bromothymol blue and methylene blue from wastewater by polyvinyl alcohol, *J. Mol. Liq.* 218 (2016) 191–197.
- H.H. Abdel Ghafar, G.A.M. Ali, O.A. Fouad, S.A. Makhlof, Enhancement of adsorption efficiency of methylene blue on Co₃O₄/SiO₂ nanocomposite, *Desalin. Water Treat.* 53 (2013) 2980–2989.
- V.K. Gupta, S. Agarwal, H. Sadegh, G.A.M. Ali, A.K. Bharti, A.S. Hamdy, Facile route synthesis of novel graphene oxide-β-cyclodextrin nanocomposite and its application as adsorbent for removal of toxic bisphenol A from the aqueous phase, *J. Mol. Liq.* 237 (2017) 466–472.
- C. Duran, D. Ozdes, A. Gundogdu, H.B. Senturk, Kinetics and isotherm analysis of basic dyes adsorption onto almond shell (*prunus dulcis*) as a low cost adsorbent, *J. Chem. Eng. Data* 56 (2011) 2136–2147.
- O.A. Habeeb, R. Kanthasamy, G.A.M. Ali, R.B.M. Yunus, Low-cost and eco-friendly activated carbon from modified palm kernel shell for hydrogen sulfide removal from wastewater: adsorption and kinetic studies, *Desalin. Water Treat.* 84 (2017) 205–214.
- H. Sadegh, G.A.M. Ali, V.K. Gupta, A.S.H. Makhlof, R. Shahryari-ghoshekandi, M.N. Nadagouda, M. Sillanpää, E. Megiel, The role of nanomaterials as effective adsorbents and their applications in wastewater treatment, *J. Nanostruct. Chem.* 7 (2017) 1–14.
- H. Sadegh, G.A.M. Ali, H.J. Nia, Z. Mahmoodi, Nanomaterial surface modifications for enhancement of the pollutant adsorption from wastewater, in: R. Nazir (Ed.), *Nanotechnology Applications in Environmental Engineering*, IGI Global, 2019, p. 143.
- H. Sadegh, G.A.M. Ali, Potential applications of nanomaterials in wastewater treatment: nanoadsorbents performance, in: A. Hussain, S. Ahmed (Eds.), *Advanced Treatment Techniques for Industrial Wastewater*, IGI Global, 2019, pp. 51–61.
- A. Mittal, J. Mittal, A. Malviya, V.K. Gupta, Adsorptive removal of hazardous anionic dye “Congo red” from wastewater using waste materials and recovery by desorption, *J. Colloid Interface Sci.* 340 (2009) 16–26.
- M.K. Purkait, A. Maiti, S. Dasgupta, S. De, Removal of Congo red using activated carbon and its regeneration, *J. Hazard Mater.* 145 (2007) 287–295.
- K. Zare, H. Sadegh, R. Shahryari-ghoshekandi, B. Maazinejad, V. Ali, I. Tyagi, S. Agarwal, V.K. Gupta, Enhanced removal of toxic Congo red dye using multi walled carbon nanotubes: kinetic, equilibrium studies and its comparison with other adsorbents, *J. Mol. Liq.* 212 (2015) 266–271.
- R. Ahmad, R. Kumar, Adsorptive removal of Congo red dye from aqueous solution using bael shell carbon, *Appl. Surf. Sci.* 257 (2010) 1628–1633.
- S. Dawood, T.K. Sen, Removal of anionic dye Congo red from aqueous solution by raw pine and acid-treated pine cone powder as adsorbent: equilibrium, thermodynamic, kinetics, mechanism and process design, *Water Res.* 46 (6) (2012) 1933–1946.
- I.D. Mall, V.C. Srivastava, N.K. Agarwal, I.M. Mishra, Removal of Congo red from aqueous solution by bagasse fly ash and activated carbon: kinetic study and equilibrium isotherm analyses, *Chemosphere* 61 (2005) 492–501.
- C. Lei, M. Pi, C. Jiang, B. Cheng, J. Yu, Synthesis of hierarchical porous zinc oxide (ZnO) microspheres with highly efficient adsorption of Congo red, *J. Colloid Interface Sci.* 490 (2017) 242–251.
- H. Sadegh, G.A.M. Ali, A.S.H. Makhlof, K.F. Chong, N.S. Alharbi, S. Agarwal, V.K. Gupta, MWCNTs-Fe₃O₄ nanocomposite for Hg(II) high adsorption efficiency, *J. Mol. Liq.* 258 (2018) 345–353.
- D. Robati, B. Mirza, R. Ghazisaeidi, M. Rajabi, O. Moradi, I. Tyagi, S. Agarwal, V.K. Gupta, Adsorption behavior of methylene blue dye on nanocomposite multi-walled carbon nanotube functionalized thiol (MWCNT-SH) as new adsorbent, *J. Mol. Liq.* 216 (2016) 830–835. ADDIN EN.REFLIST.
- H. Sadegh, G.A.M. Ali, Z. Abbasi, M.N. Nadagoud, Adsorption of ammonium ions onto multi-walled carbon nanotubes, *Stud. Chem.* 62 (2017) 233–245.
- C. Zhang, G. Wang, Y. Ji, M. Liu, Y. Feng, Z. Zhang, B. Fang, Enhancement in analytical hydrazine based on gold nanoparticles deposited on ZnO-MWCNTs films, *Sensor Actuat. B* 150 (2010) 247–253.
- A. Elaziouti, B. Ahmed, ZnO-assisted photocatalytic degradation of congo Red and benzopurpurine 4B in aqueous solution, *J. Chem. Eng. Process Technol.* 2 (2011) 1–9.
- O.A. Habeeb, K. Ramesh, G.A.M. Ali, R.M. Yunus, Experimental design technique on removal of hydrogen sulfide using CaO-eggshells dispersed onto palm kernel shell activated carbon: Experiment, optimization, equilibrium and kinetic studies, *J. Wuhan Univ. Technol.-Mater. Sci. Ed.* 32 (2017) 305–320.
- D. Robati, B. Mirza, M. Rajabi, O. Moradi, I. Tyagi, S. Agarwal, V.K. Gupta, Removal of hazardous dyes-BR 12 and methyl orange using graphene oxide as an adsorbent from aqueous phase, *Chem. Eng. J.* 284 (2016) 687–697.
- R. Verma, B. Mantri, A.K.S. Ramphal, Shape control synthesis, characterizations, mechanisms and optical properties of large scaled metal oxide nanostructures of ZnO and TiO₂, *Adv. Mater. Lett.* 6 (2015) 324–333.
- G.A.M. Ali, E.Y. Lih Teo, E.A.A. Aboelazm, H. Sadegh, A.O.H. Memar, R. Shahryari-ghoshekandi, K.F. Chong, Capacitive performance of cysteamine functionalized carbon nanotubes, *Mater. Chem. Phys.* 197 (2017) 100–104.
- D. Banerjee, P. Bhowmick, D. Pahari, S. Santra, S. Sarkar, B. Das, K.K. Chattopadhyay, Pseudo first ordered adsorption of noxious textile dyes by low-temperature synthesized amorphous carbon nanotubes, *Physica E* 87 (2017) 68–76.
- M. Rajabi, B. Mirza, K. Mahanpoor, M. Mirjalili, F. Najafi, O. Moradi, H. Sadegh, R. Shahryari-ghoshekandi, M. Asif, I. Tyagi, S. Agarwal, V.K. Gupta, Adsorption of malachite green from aqueous solution by carboxylate group functionalized multi-walled carbon nanotubes: Determination of equilibrium and kinetics parameters, *J. Ind. Eng. Chem* 34 (2016) 130–138.
- X. Xiao, F. Zhang, Z. Feng, S. Deng, Y. Wang, Adsorptive removal and kinetics of methylene blue from aqueous solution using NiO/MCM-41 composite, *Physica E* 65 (2015) 4–12.
- C. Namasivayam, D. Kavitha, Removal of Congo Red from water by adsorption onto activated carbon prepared from coir pith, an agricultural solid waste, *Dyes Pigm.* 54 (2002) 47–58.
- F.A. Pavan, S.L.P. Dias, E.C. Lima, E.V. Benvenutti, Removal of Congo red from aqueous solution by anilinepropylsilica xerogel, *Dyes Pigm.* 76 (2008) 64–69.
- M.I. Khan, S. Akhtar, S. Zafar, A. Shaheen, M.A. Khan, R. Luque, A. ur Rehman, Removal of congo red from aqueous solution by anion exchange membrane (EBTAC): adsorption kinetics and thermodynamics, *Materials* 8 (2015) 4147–4161.
- F. Ferrarini, L. Bonetto, J.S. Crespo, M. Giovanela, Removal of Congo red dye from aqueous solutions using a halloysite-magnetite-based composite, *Water Sci. Technol.* 73 (2016) 2132–2142.
- J. Sharma, B. Janveja, A study on removal of congo red dye from the effluents of textile industry using rice husk carbon activated by steam, *Rasayan J. Chem.* 4 (2008) 936–942.
- S. Bantahar, A. Dbik, M. El Khomri, N. El Messaoudi, B. Bakiz, A. Lacherai, Study of removal of Congo red by local natural clay, *Sci. Study Res.* 17 (2016) 295–307.